IOPscience iopscience.iop.org

Home Search Collections Journals About Contact us My IOPscience

An algebraic approach to the study of weakly excited states for a condensate in a ring geometry

This article has been downloaded from IOPscience. Please scroll down to see the full text article.

2005 J. Phys. A: Math. Gen. 38 8393

(http://iopscience.iop.org/0305-4470/38/39/007)

View the table of contents for this issue, or go to the journal homepage for more

Download details:
IP Address: 171.66.16.94
The article was downloaded on 03/06/2010 at 03:58

Please note that terms and conditions apply.

INSTITUTE OF PHYSICS PUBLISHING JOURNAL OF PHYSICS A: MATHEMATICAL AND GENERAL

J. Phys. A: Math. Gen. **38** (2005) 8393–8408 doi:10.1088/0305-4470/38/39/007

An algebraic approach to the study of weakly excited states for a condensate in a ring geometry

P Buonsante, R Franco and V Penna

Dipartimento di Fisica and UdR INFM, Politecnico di Torino, C.so Duca degli Abruzzi 24, I-10129 Torino, Italy

Received 8 June 2005, in final form 27 July 2005
Published 14 September 2005
Online at stacks.iop.org/JPhysA/38/8393

Abstract

We determine the low-energy spectrum and the eigenstates for a two-bosonic mode nonlinear model by applying the Inönü–Wigner contraction method to the Hamiltonian algebra. This model is known to well represent a Bose–Einstein condensate rotating in a thin torus endowed with two angular-momentum modes as well as a condensate in a double-well potential characterized by two space modes. We consider such a model in the presence of both an attractive and a repulsive boson interaction and investigate regimes corresponding to different values of the inter-mode tunnelling parameter. We show that the results ensuing from our approach are in many cases extremely satisfactory. To this end, we compare our results with the ground state obtained both numerically and within a standard semiclassical approximation based on $su(2)$ coherent states.

PACS numbers: 03.75.Fd, 03.65.Sq, 03.75.Lm

1. Introduction

The dynamics of a bosonic fluid rotating within a thin torus and, particularly, the study of the properties relevant to its weakly excited states have received recently much attention [1–5] due to the rich phenomenology that characterizes such a system. For example, the quantization of fluid circulation is shown [3] to disappear whenever the physical parameters cause the hybridization of condensate ground state over different angular-momentum (AM) states. A similar effect is found in the mean-field dynamics of the condensate wavefunction on a circle [4], where the circulation loses its quantized character when the system is in the soliton regime. The rotating fluid exhibits low-energy AM quantum states (corresponding to the presence of plateaus of quantized circulation) that determine the hybridization effect by a suitable tuning of the model interaction parameters [3]. In the simplest possible case, the model exhibits two momentum (bosonic) modes associated with two AM states (the ground state and the first excited state) of the fluid. An almost identical model [6–13] has been studied thoroughly in the recent years within Bose–Einstein condensates (BEC) physics, where a condensate is

 © 2005 IOP Publishing Ltd Printed in the UK

distributed in two potential wells that exchange bosons via tunnelling effect. The two-well model $H = U\left(n_0^2 + n_1^2\right) - \Delta(n_0 - n_1)/2 - V_0\left(a_0 a_1^+ + a_1 a_0^+\right)$, where a_0, a_1 are bosonic space modes and $n_i = a_i^+ a_i$, displays hybridized states when the well-depth imbalance vanishes ($\Delta = 0$).

For both models the energy regime of interest is that corresponding to the ground state or weakly excited states. In this respect, many authors have tried to develop approximation schemes able to provide a satisfactory analytical description of the low-energy spectrum and of its states. The nonlinear character of the model Hamiltonian entails a difficult diagonalization process unless one resorts to numerical calculations. In this case, the exact form of the spectrum is obtained quite easily. However, for N-well systems such as condensate arrays described by the Bose–Hubbard model, Josephson-junction arrays and, in general, N-mode bosonic systems [14, 15], the exact diagonalization requires a computational effort rapidly increasing with N. This motivates the interest in developing effective, analytical approximation methods able to solve the diagonalization problem.

The present work has been inspired by papers [2, 3] where, among the various issues considered, the structure of the ground state of a ring condensate (within a two-AM-mode approximation of the bosonic quantum field) has been studied. As to the closely related two-well boson model, the same problem has been investigated in [16] within the Hermitian phase operator method. In order to obtain a satisfactory description of the system ground state as well as of the weakly excited states for the two-mode model, we implement, in the present paper, an algebraic approach based on the *Inönü–Wigner contraction* method [17]. This method allows one to simplify the algebraic structure of the Hamiltonian reducing the latter in a form apt to perform a completely analytic derivation of its spectrum. A well-defined limiting procedure, mapping the original Hamiltonian generating algebra to a simpler algebra, often succeeds in reducing the nonlinear terms to a tractable form. These terms, originated by the boson–boson interaction and thus occurring in any model inherent in BEC dynamics, are known to make the Hamiltonian diagonalization a hard task. Such a technique and the effect of simplifying the algebraic structure of model Hamiltonians, has found a wide application in many fields of theoretical physics. It is well illustrated, for example, in [18] where it is applied to study collective phenomena in nuclear models.

The contraction-method approach (CMA)—namely the contraction procedure and the ensuing approximation of weakly excited states—works well for the spectrum sectors where the energy levels are close to the minima and the maxima of the classical Hamiltonian and thus seems suitable for studying the low-energy regime of two-mode nonlinear models. The results obtained within the CMA in sections 2 and 3 will be compared both with the exact spectrum calculated numerically and with an alternative approach based on the coherent-state semiclassical approximation (CSSA) reviewed in section 4.

We consider N interacting bosons with mass m whose boson–boson interaction can be either attractive or repulsive. These are confined in a narrow annulus whose thickness $2r$ is much smaller than the annulus radius R. Bosons are also acted upon by an external potential which causes inter-mode tunnelling. Particularly, the rotating fluid with an attractive interaction can be shown to be equivalent to the two-well model of repulsive bosons introduced previously. In the coordinate frame of the potential rotating with angular velocity ω and with the z-axis parallel to the total angular momentum $L_{\mathrm{tot}} = L_z$, the bosonic-field Hamiltonian reads

$$\hat{H}_{bf} = \int \mathrm{d}^3\mathbf{r}\hat{\psi}_{\mathbf{r}}^+ \left[\frac{P^2}{2m} - \omega L_z + V_{\mathrm{ext}}(\mathbf{r})\right]\hat{\psi}_{\mathbf{r}} + \frac{1}{2}\int\int \mathrm{d}^3\mathbf{r}\,\mathrm{d}^3\mathbf{s}\hat{\psi}_{\mathbf{r}}^+\hat{\psi}_{\mathbf{s}}^+ U(|\mathbf{r}-\mathbf{s}|)\hat{\psi}_{\mathbf{s}}\hat{\psi}_{\mathbf{r}}$$

where $\hat{\psi}_{\mathbf{r}} = \hat{\psi}(\mathbf{r})$ $\left(\hat{\psi}_{\mathbf{r}}^+\right)$ is the destruction (creation) boson field operator at $\mathbf{r}$. V_{ext} is the confining potential. At a low temperature, the interaction between dilute bosons is well

represented by the Fermi contact interaction which entails the standard approximation $U(|\mathbf{r}-\mathbf{s}|) \simeq (4\pi\hbar^2 a/m)\delta(|\mathbf{r}-\mathbf{s}|)$, where a is the s-wave scattering length [2].

1.1. Two-mode approximation

The two-mode approximation involves only the first two states of AM, with eigenvalue equations $L_z\psi_0(\mathbf{r}) = 0$ and $L_z\psi_1(\mathbf{r}) = \hbar\psi_1(\mathbf{r})$. Field operator $\hat{\psi}(\mathbf{r})$ in the two-mode basis of L_z is thus written as $\hat{\psi}(\mathbf{r}) \simeq a_0\psi_0(\mathbf{r}) + a_1\psi_1(\mathbf{r})$, where a_0, a_1 are bosonic operators and the validity of the two-mode approximation requires the condition $0 < \omega < 2\omega_c$ (greater angular velocities would involve other angular-momentum states). Within such an approximation [6, 9] and considering a thin torus ($r \ll R$) $\hat{H}_{bf}$ reduces to [2] $H = g\big(n_0^2 + n_1^2 - n_0 - n_1 + 4n_0n_1\big)/2 - \Delta\hbar n_1/2 - V_0\big(a_1^+a_0 + a_0^+a_1\big)$, where $n_i = a_i^+a_i$, $\Delta = 2\hbar(\omega - \omega_c)$, while $\omega_c = \hbar/(2mR^2)$, $g = 2\hbar^2 a/(mR\pi r^2)$ and V_0 are the critical angular frequency, the mean interaction energy per particle and the asymmetry of potential $V_{\text{ext}} = V_0(\mathrm{e}^{\mathrm{i}\theta} + \mathrm{e}^{\mathrm{i}\theta})$, respectively. In the Schwinger picture [7] of algebra $su(2)$ H further simplifies becoming, up to a constant term,

$$H = -gJ_3^2 - 2V_0J_1 - \Delta J_3, \tag{1}$$

where $J_3 = (n_1 - n_0)/2$, $J_1 = (J_+ + J_-)/2$, $J_2 = (J_+ - J_-)/2\mathrm{i}$ and $J_+ = a_1^+a_0$, $J_- = (J_+)^+$. Such generators satisfy the commutators $[J_r, J_s] = \mathrm{i}\epsilon_{rsv}J_v$ (ϵ_{rsv} is the antisymmetric symbol) and commute with the total boson number operator $n_1 + n_0$ $\big(n_i = a_i^+a_i\big)$ whose eigenvalue N is connected with the $su(2)$-representation index J by $J = 2N$. In such a scheme, the AM states are defined by

$$|J; m\rangle := |n_0\rangle \otimes |n_1\rangle, \qquad n_1 = J + m, \qquad n_0 = J - m,$$

where the J_3-basis states satisfy the eigenvalue equations $J_3|J; m\rangle = m|J; m\rangle$ and $J_4|J; m\rangle = J|J; m\rangle$, the index J being the eigenvalue of $J_4 = (n_1 + n_0)/2$. The positive (negative) sign of g in model (1) implies that the effective interaction between bosons is repulsive (attractive). The conditions of weak asymmetry and interaction ensuring the validity of the model [2] are given by $|V_0| \ll \hbar\omega_c$ and $|g| \ll \hbar\omega_c$. The simple spin form of Hamiltonian (1) evidences how the attractive model ($g < 0$) coincides with a (repulsive) two-site Bose–Hubbard Hamiltonian [7, 11] modelling two potential wells of different depth that share $N = 2J$ bosons and exchange them via tunnel effect. The N-boson physical states can be written as $|\psi\rangle = \sum_{m=-J}^{J} X_m|J; m\rangle$, while the Schrödinger equation $(\mathrm{i}\hbar\partial_t - H)|\psi\rangle = 0$ can be expressed in components as

$$\mathrm{i}\hbar\dot{X}_m = (-gm^2 - m\Delta)X_m - V_0\big[R_{m+1}^J X_{m+1} + R_m^J X_{m-1}\big],$$

once the symbol $R_m^J = [(J+m)(J-m+1)]^{1/2}$ has been defined. It is worth noting that the study of the algebraic structure characterizing the second-quantized Hamiltonian for a condensate trapped in two potential wells has received much attention in the literature. In the seminal work [14] and in [15], in particular, such Hamiltonian has been shown to reduce, within a standard mean-field approach, to the sum of mode Hamiltonians describing the momentum conservation in the presence of inter-well boson exchange due to the tunnelling. Each mode Hamiltonian is written in terms of operators a_k, a_{-k} ($\pm k$ are the momentum modes) and can be reformulated as a linear combination of $su(1,1)$ generators. In model (1) the momentum conservation is explicitly violated since one of the modes takes into account the fluid rotation. This fact entails that the previous Schwinger realization of algebra $su(2)$, rather than the algebra $su(1,1)$ connected with the momentum conservation, characterizes the system.

In our analysis the dimensionless mean value per boson of the angular momentum $\langle l_z\rangle = \langle L_z\rangle/\hbar N$ (where the notation $\langle A\rangle = \langle\psi|A|\psi\rangle$ has been introduced) represents an important quantity. The angular momentum, in fact, expressed as

$$\langle l_z\rangle = \sum_{m=-J}^{J} \frac{J+m}{2J}|X_m|^2 = \left(\frac{1}{2} + \frac{\langle J_3\rangle}{2J}\right), \tag{2}$$

relates the macroscopic behaviour of the rotating condensate to the minimum-energy state properties through the ground-state components X_m. In what follows, we consider the spectral properties of model (1) both in the attractive case ($g < 0$)

$$H_a = |g|J_3^2 - 2V_0J_1 - \Delta J_3, \tag{3}$$

and in the repulsive case ($g > 0$)

$$H_r = -\big(|g|J_3^2 + 2V_0J_1 + \Delta J_3\big). \tag{4}$$

It is worth noting that the study of the ground-state properties of the repulsive case is closely related to the study of the maximum-energy state for the attractive Hamiltonian. In fact, after the substitutions $V_0 \to -V_0$ and $\Delta \to -\Delta$, the repulsive Hamiltonian is identical to the attractive one up to a factor (-1). Since these two changes can be effected in a unitary way by means of transformations $\mathrm{e}^{+\mathrm{i}\pi J_3}J_1\,\mathrm{e}^{-\mathrm{i}\pi J_3} = -J_1$ and $\mathrm{e}^{+\mathrm{i}\pi J_1}J_3\,\mathrm{e}^{-\mathrm{i}\pi J_1} = -J_3$, respectively, the spectra of H_r and H_a turn out to satisfy the equation $\mathrm{spect}[H_a(V_0,\Delta)] = -\mathrm{spect}[H_r(-V_0,-\Delta)]$. Concerning the parameter Δ of Hamiltonian (1), we note that the constraint $0 \leqslant \omega \leqslant 2\omega_c$ implies the inequality $-2\hbar w_c < \Delta < 2\hbar w_c$. The definition of the further parameters $\gamma = J|g|/2\hbar w_c$, $\tau = V_0/J|g|$ allows one to better characterize the regimes of the rotational dynamics as well as the conditions of validity of the present model. Parameter γ (representing the ratio of the self-interaction energy per particle to the single-particle energy-level spacing) should satisfy the inequalities $2\gamma \ll J$, $\tau \ll 1/2\gamma$, owing to the conditions $|g| \ll \hbar\omega_c$ and $V_0 \ll \hbar\omega_c$, respectively. Both these conditions can be satisfied if $J = N/2$ is not excessively large [2]. Moreover, parameter $\tau = V_0/(J|g|)$ allows one to distinguish, in both the attractive and repulsive case, three regimes:

- the Fock regime, where $|g| \gg V_0J$ entails $\tau \ll 1/J^2$;
- the Josephson regime, where $V_0/J \ll |g| \ll V_0J$ entails $1/J^2 \ll \tau \ll 1$;
- the Rabi regime, where $|g| \ll V_0/J$ entails $\tau \gg 1$.

We note that the condition of weak asymmetry $|V_0| \ll \hbar\omega_c$ given by $\tau \ll 1/2\gamma$ appears to be compatible with the first two regimes and with part of the Rabi regime.

2. The Inönü–Wigner contraction in the attractive case

We introduce a simple algebraic approach for studying the low-energy spectrum of Hamiltonians (3) and (4) for large J whose essence consists in simplifying the nonlinearity due to the term J_3^2. The Inönü–Wigner contraction [19] supplies a method for mapping some given algebraic structure in a new one, as the result of a singular limiting process. The contraction is realized by defining a set of new operators h_i as linear combinations $h_i = \sigma_i I + \Sigma_k c_{ik}g_k$ of the generators g_k of a given algebra (identified by its commutators $[g_r, g_s] = \varepsilon_{rsk}g_k$) and of the identity operator I. Selecting an appropriate parametrization $c_{ik}(x)$ of the linear-map coefficients, the contraction enacted by means of the limit $x \to 0$ is able to generate the new algebraic structure $[h_i, h_j] = e_{ijk}h_k$ whose structure constants $\{e_{ijk}\}$ differ from the original ones $\{\varepsilon_{rsk}\}$. For the algebra $su(2)$ the contraction of the algebra mapping is driven by

$x = 1/\sqrt{J}$ (with $J \to \infty$) and generates, in this limit, the harmonic oscillator (namely the Heisenberg–Weyl) algebra [20].

The classical study of attractive ($g < 0$) Hamiltonian $H_a = |g|J_3^2 - 2V_0J_1 - \Delta J_3$ developed in (appendix A) demonstrates (see formula (A.2)) how $J_1 \simeq +J$, $J \gg |J_2|, |J_3| \simeq 0$, at low energies. This suggests the correct way to implement the contraction scheme. In the present attractive case we can build the following transformation,

$$h_1 = J_1 - I/x^2, \qquad h_2 = xJ_2, \qquad h_3 = xJ_3, \tag{5}$$

where $J_4 = JI$. The Inönü–Wigner contraction is realized when such a x-dependent transformation is considered in the (singular) limit $J = 1/x^2 \to \infty$. In this case the objects $\{J_i\}$ (with $i = 1, 2, 3, 4$), defining algebra $u(2)$, transform into the new objects $\{h_i, I\}$ (with $i = 1, 2, 3$) that satisfy the following commutation relations:

$$[h_2, h_3] = \mathrm{i}(x^2h_1 + I) \to \mathrm{i}I, \qquad [h_1, h_2] = x[J_1, J_2] = \mathrm{i}h_3, \tag{6}$$

$$[h_1, h_3] = x[J_1, J_3] = -\mathrm{i}h_2, \qquad [h_i, I] = 0. \tag{7}$$

In the limit $x = 1/\sqrt{J} \to 0$, the latter reproduce the commutation relations of Weyl–Heisenberg algebra: $[q, p] = \mathrm{i}, [n, q] = -\mathrm{i}p, [n, p] = \mathrm{i}q, n = (q^2 + p^2)/2$, thereby suggesting the identifications $h_1 \equiv -n, h_2 \equiv -p, h_3 \equiv q$. By combining the latter with definitions (5) we find that the contraction gives $J_1 \to J - n, J_2 \to -\sqrt{J}p, J_3 \to \sqrt{J}q$. Correspondingly, Hamiltonian H_a becomes $H_a = |g|Jq^2 + 2V_0n - 2V_0J - \Delta\sqrt{J}q$, which, by defining $\Omega = [1 + 1/\tau]^{1/2}$ and $Q = q - \chi$ with $\chi = \sqrt{J}\Delta/2V_0\Omega^2$, and $\tau = V_0/J|g|$, reduces to the form

$$H_a = V_0\left[p^2 + \Omega^2Q^2 - 2J - \frac{J\Delta^2}{4V_0^2\Omega^2}\right]. \tag{8}$$

Since $p^2 + \Omega^2Q^2 = 2\Omega(n + 1/2)$ is diagonalized by the harmonic-oscillator eigenstates $\Psi_n(Q) = \langle Q|E_n\rangle = N_n\,\mathrm{e}^{-\Omega Q^2/2}H_n(\sqrt{\Omega}Q)$, the eigenvalues of Hamiltonian (8) are found to be

$$E_n = V_0\left[2\Omega(n + 1/2) - 2J - \frac{J\Delta^2}{4\Omega^2V_0^2}\right]. \tag{9}$$

The corresponding eigenvalue equation $H_a|E_n\rangle = E_n|E_n\rangle$ in the J_3 basis, where $|E_n\rangle = \Sigma_m X_n(m)|J, m\rangle$, can be written as $\Sigma_m(H_a)_{\ell m}X_n(m) = E_nX_n(\ell)$ with $(H_a)_{\ell m} = \langle J, \ell|H_a|J, m\rangle$. In the limit $J \gg 1$, equation $J_3|J, m\rangle = m|J, m\rangle$ is replaced by $q|J, m\rangle = (m/\sqrt{J})|J, m\rangle$. Therefore the eigenvalue $m/\sqrt{J}$ can be seen as a continuous variable which naturally identifies with the variable $q \simeq J_3/\sqrt{J}$ used within the approximation scheme just discussed. The component version of the eigenvalue equation for H_a then reduces (see [20] for details) to the equation $H_a(Q, p)\Psi_n(Q) = E_n\Psi_n(Q)$ solved above. Components $X_m(E_n)$ thus appear to be given by $X_m(E_n) = \Psi_n(Q)$ that entail the explicit expression for the eigenstates

$$|E_n\rangle = \Sigma_m X_m(E_n)|J; m\rangle, \qquad X_m(E_n) = N_nH_n(\sqrt{\Omega}Q)\,\mathrm{e}^{-\Omega Q^2/2} \tag{10}$$

with $Q = m/\sqrt{J} - \chi$. The normalization constants N_n are determined through the condition $\langle E_n|E_n\rangle = 1$ implying that

$$1 = \sum_{m=-J}^{J} X_m^2(E_n) \simeq \int_{-\infty}^{\infty} \mathrm{d}q\,\frac{N_n^2}{\sqrt{J}}H_n^2[\sqrt{\Omega}(q - \chi)]\,\mathrm{e}^{-\Omega(q-\chi)^2}, \tag{11}$$

where $\pm J$ has been replaced with $\pm\infty$. Such an approximation is acceptable until the condition

$$|\chi| < \sqrt{J} - \sqrt{2n/\Omega}, \tag{12}$$

evinced from the interval containing the Hermite-polynomial zeros, is fulfilled. Excluding the case $\tau \gg 1$, this condition is always valid provided $n \ll J$. Thus constants N_n are given by $N_n = [(J\Omega)^{1/2}/(\pi^{1/2}2^n n!)]^{1/2}$.

Another important check concerns the possibility of considering $m/\sqrt{J}$ as a continuous variable. The characteristic scale is established by the Gaussian deviation $\sqrt{2/\Omega}$ which must be compared with the smallest variation $1/\sqrt{J}$ of q. The resulting condition $1/\sqrt{J} < \sqrt{2/\Omega}$ can be written as

$$1 < \frac{2J}{\Omega} = 2J\left[\frac{V_0}{V_0 + J|g|}\right]^{1/2} = 2J\left[\frac{\tau}{\tau+1}\right]^{1/2}.$$

While in the Rabi and Josephson regimes ($1/J^2 \ll \tau$) the latter is fully satisfied, in the Fock regime, where $\tau \ll 1/J^2$, such a condition is violated. We note that for $\tau \simeq 1/J^2$ (namely $|g| \approx JV_0$) a unique component X_m appears to contribute to states $|E_n\rangle$ since the Gaussian amplitude becomes very small. For example, in the case of the ground state one has

$$|E_0\rangle = \Sigma_m N_0\, \mathrm{e}^{-\frac{\Omega}{2}\left(\frac{m}{\sqrt{J}}-\chi\right)^2}|J,m\rangle \simeq N_0\, \mathrm{e}^{-\frac{\Omega}{2}\left(\frac{m_*}{\sqrt{J}}-\chi\right)^2}|J,m_*\rangle, \tag{13}$$

where m_* is the integer closest to $\sqrt{J}\chi \simeq \Delta/2|g|$. Nevertheless, in the special case when $\Delta/2|g| = m_* + 1/2$, the two states $|J,m_*\rangle$ and $|J,m_*+1\rangle$ equally contribute to $|E_0\rangle$ which is given by

$$|E_0\rangle \simeq N_0\, \mathrm{e}^{-\frac{\Omega}{8J}}(|J,m_*\rangle + |J,m_*+1\rangle). \tag{14}$$

To summarize, we note how the ground state $|E_0\rangle$ is essentially formed by a unique component corresponding to $|J,m_*\rangle$ in the whole parameter range $m_* - 1/2 < \Delta/2|g| < m_* + 1/2$. The resonance of the system between two equivalent states crops up whenever $\Delta/|g|$ assumes integer values given by $\Delta/|g| \equiv 2m+1$ with $-J \leqslant m \leqslant J$. Such a condition can be implemented by varying Δ with $|g| = \text{const}$ thus leaving Ω unchanged.

2.1. Comparison of different regimes

For $\tau > 1/J^2$ (Rabi and Josephson regimes), one easily calculates the dimensionless mean AM per boson $\langle l_z\rangle$ based on state $|E_0\rangle$, as given by formula (10), and exploiting the normalization integral (11). Recalling that $\langle J_3\rangle = \sum_{m=-J}^{J} m X_m^2(E_0)$, one finds that

$$\langle l_z\rangle = \frac{1}{2}\left(1 + \frac{\langle J_3\rangle}{J}\right) \simeq \frac{1}{2} + \frac{\tau\Delta}{4V_0(1+\tau)}, \qquad \langle J_3\rangle \simeq \sqrt{J}\chi = \frac{J\tau\Delta}{2V_0(1+\tau)}, \tag{15}$$

where $\langle J_3\rangle$ matches exactly formula (A.3) obtained in the classical study of the attractive model. This result cannot be used in the Fock regime where the ground state has, at most, either one or two dominating components. In the other two regimes, the second of equations (15) entails the further consistence condition

$$-1 \leqslant \langle J_3\rangle/J = \tau\Delta/[2V_0(1+\tau)] \leqslant +1, \tag{16}$$

which has to be verified in each regime. In view of the condition $|\langle J_3\rangle| \ll J$ required to implement the contraction procedure, formula (16) should be imposed in the stronger version $|\tau\Delta/[2V_0(1+\tau)]| \ll 1$. However, the numerical (exact) determination of the ground state for various choices of parameters reveals that our approximate procedure works well also in the case when $|\tau\Delta/[2V_0(1+\tau)]|$ is not particularly small.

Fock regime. The main feature of this case ($\tau \ll 1/J^2$) is that the mean dimensionless AM per boson is a step function of Δ (as to this well-known effect see, e.g., [3]). If one simplifies the form of states (13) and (14) by setting $|E_0\rangle = |J,m\rangle$ and $|E_0\rangle = (|J,m\rangle + |J,m+1\rangle)/\sqrt{2}$

in correspondence to the appropriate values of Δ, the dimensionless mean AM per boson is found to be

$$\langle l_z\rangle = \frac{1}{2} + \frac{m}{2J}, \qquad \langle l_z\rangle = \frac{1}{2} + \frac{m}{2J} \pm \frac{1}{4J},$$

for $m - 1/2 < \Delta/2|g| < m + 1/2$ and $\Delta/2|g| = m \pm 1/2$, respectively, corresponding to the two choices of the Fock ground state $|E_0\rangle$. This illustrates the AM step character (related to the Hess–Fairbank effect) as well as its 'singular' behaviour when $\Delta/2|g| = m \pm 1/2$. Note that considering the simplified form for $|E_0\rangle$ is equivalent to assuming the net predominance of one or two components. The results just found are consistent with the limit $\tau \to 0$, where $H_a = |g|J_3^2 - \Delta J_3$ can be diagonalized in a direct way.

Josephson and Rabi regimes. In these cases $1/J^2 \ll \tau \ll 1$ and $1 \ll \tau$, respectively. Based on the above formulae, one finds that $\langle J_3\rangle \simeq J\tau\Delta/2V_0$ (the Josephson case) and $\langle J_3\rangle \simeq J\Delta/2V_0$ (the Rabi case) giving the mean dimensionless AM per boson

$$\langle l_z\rangle = \frac{1}{2}\left[1 + \frac{\tau\Delta}{2V_0}\right], \qquad \langle l_z\rangle = \frac{1}{2}\left[1 + \frac{\Delta}{2V_0}\right],$$

respectively. Owing to formulae (15) and (16), in the Josephson case, the range of parameter Δ is $[-2J|g|, \leqslant 2J|g|]$. For this regime, the further condition (12) reduces to $(2n\tau^{1/2}/J)^{1/2} + (\Delta/2J|g|) < 1$. In the Rabi case, condition (16) on $\langle J_3\rangle$ entails that Δ ranges in $[-2J\tau|g|, 2J\tau|g|]$ $(2J\tau|g| = 2V_0)$ which is, in principle, much larger than the range allowed in the Josephson case. Considering once more condition (12) gives in the Rabi case $(2n\tau^{1/2}/J)^{1/2} + (\Delta/2V_0) < 1$. One easily checks that weakly excited states $|E_n\rangle$ satisfy the conditions on the restricted range of Δ provided $n \ll J$, and $|\Delta| \ll 2J|g|$, $|\Delta| \ll 2V_0$ in the Josephson case and in the Rabi case, respectively. In both cases the latter inequalities represent condition (16) in its stronger version.

3. The Inönü–Wigner contraction in the repulsive case

The classical study of repulsive Hamiltonian $H_r = -\big(|g|J_3^2 + 2V_0J_1 + \Delta J_3\big)$, discussed in (appendix A), shows that, with $\tau = V_0/J|g| > 1$ (the Rabi regime), the energy minimum is such that $J_1 = J, J_2 = J_3 = 0$. As shown by equation (A.5), a generic state near the minimum is such that $J_1 \simeq J, |J_2|, |J_3| \ll J$. In the Fock/Josephson regimes, where $\tau = V_0/J|g| < 1$, Hamiltonian H_r displays two minimum-energy states (see equation (A.7)) entailing low-energy configurations characterized by $J_3 \simeq \pm J, |J_2|, |J_1| \ll J$.

3.1. The repulsive regime with $\tau > 1$

In the Rabi regime ($\tau > 1$), the CMA valid for the attractive model can be implemented again. Then assuming h_1, h_2, h_3 as in formulae (5) the result of the contraction gives $J_1 \to J - n$, $J_2 \to -\sqrt{J}p$ and $J_3 \to \sqrt{J}q$, which reduce H_r to a quadratic form. By defining $Q = q - c$, with $c = \sqrt{J}\Delta/(2V_0W^2)$, the final form of H_a is found to be

$$H_a = V_0\left[p^2 + W^2Q^2 - 2J - \frac{J\Delta^2}{4V_0^2W^2}\right]. \tag{17}$$

Since the eigenvalues of $p^2 + W^2q^2$ are $\Lambda_n = 2W(n + 1/2)$, the spectrum of H_r is

$$E_n = V_0\left[2W(n + 1/2) - 2J - \frac{J\Delta^2}{4V_0^2W^2}\right]. \tag{18}$$

As in the attractive case, the eigenfunctions $\Phi_n(Q)$ of Hamiltonian (17) allow one to determine components X_m through the formula $X_m(E_n) = \Phi_n(Q)$. The energy eigenstates turn out to be

$$|E_n\rangle = \Sigma_m X_m(E_n)|J; m\rangle, \qquad X_m(E_n) = N_n H_n(\sqrt{W}\,Q)\,\mathrm{e}^{-\frac{WQ^2}{2}}, \tag{19}$$

with $Q = m/\sqrt{J} - c$. This description is valid if the conditions on the Gaussian deviation and the Hermite-polynomial zeros $1/\sqrt{J} < \sqrt{2/W}$ and $|c| < \sqrt{J} - \sqrt{2n/W}$, respectively, which can be rewritten as $1 < 2J\tau/(\tau - 1)$ and $|\Delta|\tau/[2V_0(\tau - 1)] < 1 - \{2n\tau^{1/2}/[J(\tau - 1)^{1/2}]\}^{1/2}$, are satisfied. For $\tau \gg 1$, the first condition is fulfilled, while the second one gives $\Delta/2V_0 < 1 - \sqrt{2n/J}$. The latter is satisfied if $\Delta/2V_0 < 1$. Weakly excited states $|E_n\rangle$ with $n > 0$ can be also considered provided $J \gg 2n$. Under such conditions, the mean dimensionless AM per boson is a linear function of Δ

$$\langle l_z\rangle = \frac{1}{2}(1 + \langle J_3\rangle/J) = \frac{1}{2}\left[1 + \frac{\Delta\tau}{2V_0(\tau - 1)}\right], \qquad \langle J_3\rangle = c\sqrt{J} = J\Delta\tau/2V_0(\tau - 1),$$

giving $\langle l_z\rangle \simeq (1 + \Delta/2V_0)/2$ for $\tau \gg 1$. Note that $\langle J_3\rangle$ coincides with formula (A.6) for the minimum of the classical repulsive model and that, in the Rabi regime, $\langle l_z\rangle$ has the same form both for attractive bosons ($g < 0$) and for repulsive bosons ($g > 0$).

3.2. The repulsive case with $\tau < 1$

In this case, the classical ground-state configuration corresponds to two minima. The contraction scheme can be implemented in two ways by assuming $h_2 = xJ_2, h_1 = xJ_1$ and $h_3 = J_3 \mp I/x^2$ which entails $[h_1, h_2] = \pm \mathrm{i}x^2 h_3, [h_2, h_3] = \mathrm{i}h_1$, and $[h_3, h_1] = \mathrm{i}h_1$. Note that $h_3 = J_3 \mp I/x^2$ allows us to describe the two classical minima by further selecting a suitable definition for h_3. The result of the contractions demonstrates the two possible choices

$$h_3 = -n, \qquad h_2 = J_2/\sqrt{J} \to p, \qquad h_1 = J_1/\sqrt{J} \to q, \tag{20}$$

and

$$h_3 = +n, \qquad h_2 = J_2/\sqrt{J} \to -p, \qquad h_1 = J_1/\sqrt{J} \to q, \tag{21}$$

that are naturally associated with the J_3-positive and J_3-negative minimum, respectively. The repulsive Hamiltonian $H_r = -\left(|g|J_3^2 + 2V_0J_1 + \Delta J_3\right)$ thus can be cast in the two (local) forms

$$H_r = -|g|\left[J^2 - 2Jn + 2\tau J^{3/2}q + \frac{s\Delta}{|g|}(J - n)\right], \tag{22}$$

where $s = \pm$ recalls the presence of two minima. Note that H_r could be diagonalized by means of the procedure used in the attractive case, provided one adopts the rotated basis $\{|m\rangle_1 = \exp(-\mathrm{i}\pi J_2/2)|m\rangle\}$ of J_1 and regards the q eigenvalues $m/\sqrt{J}$ as a continuous index. Unfortunately, while the evaluation of the energy eigenvalues is very easy in the 'rotated' J_1 basis $\{|m\rangle_1 = \exp(-\mathrm{i}\pi J_2/2)|m\rangle, |m| \leqslant J\}$, the eigenstates must be counter-rotated to recover the J_3-basis representation that we have adopted in the other cases/regimes. This is a difficult problem in that recovering the eigenstates description in the J_3 basis requires that the transformation matrix element $\langle m'|\exp(-\mathrm{i}\pi J_2/2)|m\rangle$ is calculated explicitly and is formulated in the limit where $m/\sqrt{J}$ is a continuous index.

To skip this problem, we observe that, owing to formulae (20) and (21) derived by the contraction procedure, $J_3^2 + J_2^2 + J_1^2 = J(J+1) \simeq J^2$ can be rewritten as $J_3^2 \simeq 2Jn - J^2$ while $J_3 = \pm(J - n)$. We thus obtain the linearized expression $J_3^2 \simeq -J^2 \pm 2JJ_3$. Hamiltonian (22) reduces to $H_r = -|g|[-J^2 \pm 2JJ_3 + 2\tau JJ_1 + (\Delta/|g|)J_3]$, whose digonalization is rather simple owing to the linear dependence on $su(2)$ generators. Rewriting the latter

as $H_r^{\pm} = |g|[J^2 \mp (2J \pm \delta)J_3 - 2\tau JJ_1]$ where $\delta = \Delta/|g|$, the unitary transformations $U_{\pm} = \exp(\mp \mathrm{i}J_2\phi_{\pm})$ entail

$$H_r^{\pm} = |g|\big[J^2 \mp R_{\pm}U_{\pm}J_3U_{\pm}^{+}\big], \tag{23}$$

with $R_{\pm} = \sqrt{(2J \pm \delta)^2 + 4\tau^2J^2}$. The action of $U_{\pm}$ is given by

$$U_-J_3U_-^{\dagger} = J_3\cos\phi_- - J_1\sin\phi_-, \qquad U_+J_3U_+^{\dagger} = J_3\cos\phi_+ + J_1\sin\phi_+, \tag{24}$$

where angles $\phi_{\pm}$ are defined by $\mathrm{tg}\phi_- = 2\tau J/(2J - \delta)$, $\mathrm{tg}\phi_+ = 2\tau J/(2J + \delta)$. The energy spectrum is thus represented by the eigenstates and the eigenvalues

$$\big|E_m^{\pm}\big\rangle = U_{\pm}|m\rangle, \qquad E_m^{\pm} = |g|\big[J^2 \mp m\sqrt{(2J \pm \delta)^2 + 4\tau^2J^2}\big], \tag{25}$$

respectively. One should recall that, within the present approximation scheme, these eigenvalues are significant for $|m| \approx J$. Moreover, we note that $U_{\pm} \to \mathbf{1}$ for $\tau \to 0$ thus reproducing the correct spectrum of the uncoupled model. The eigenvalues corresponding to the energy minima are obtained by setting $m = -J$ and $m = +J$ for H_r^- and H_r^+, respectively, and read

$$E_M^{\pm}(\delta) := E_{\pm J}^{\pm} = |g|\big[J^2 - J\sqrt{(2J \pm \delta)^2 + 4\tau^2}\big]. \tag{26}$$

The choice of the signs $\pm$, and thus the recognition of the lowest energy states, is related to the sign of δ. This is discussed below.

The states associated with eigenvalues (26) take the form of $su(2)$ coherent states [21]. The standard $su(2)$ picture of such states, also known as Bloch states, is given by

$$|-J, \xi\rangle = \mathrm{e}^{\xi J_+ - \xi^* J_-}|-J\rangle = \sum_{s=0}^{2J} \frac{C_{Js}z^s|s - J\rangle}{(1 + |z|^2)^J} \tag{27}$$

with $C_{Js} = \sqrt{(2J)!/s!(2J - s)!}$, while the coherent-state labels $z = |z|\,\mathrm{e}^{\mathrm{i}\theta}$ and $\xi = |\xi|\,\mathrm{e}^{\mathrm{i}\theta}$ are such that $|z| = \mathrm{tg}|\xi|$, $z \in \mathbf{C}$. Since the minimum-energy states have the form

$$\big|E_M^{\pm}\big\rangle = \mathrm{e}^{\mp \mathrm{i}J_2\phi_{\pm}}|\pm J\rangle, \tag{28}$$

where $\mp \mathrm{i}J_2\phi_{\pm} = \mp(\phi_{\pm}/2)(J_+ - J_-)$, the link with the coherent-state picture is almost immediate. Upon setting $\xi = \mp\phi_{\pm}/2$, the corresponding z reads $z = \mp\mathrm{tg}(\phi_{\pm}/2) = \mp 2\tau J/(2J \pm \delta)$. In view of this, eigenstate $|E_M^-\rangle$ takes the new form

$$|E_M^-\rangle = \cos^{2J}(\phi_-/2)\sum_{s=0}^{2J} C_{Js}\mathrm{tg}^s(\phi_-/2)|s - J\rangle. \tag{29}$$

If $\delta < 0$, state $|E_M^-(\delta)\rangle$ (we make explicit the dependence from δ to illustrate clearly the difference between the absolute minimum and the local minimum) corresponds to the lowest energy state with eigenvalue $E_M^-(\delta) = |g|\big[J^2 - J\sqrt{(2J + |\delta|)^2 + 4\tau^2}\big]$, since $E_M^-(\delta) < E_M^+(\delta)$ (see equation (26)). The remaining state $\big|E_M^+(\delta)\big\rangle$ represents the local minimum found in the classical dynamics. In the opposite case $\delta > 0$, the lowest energy state identifies with $\big|E_M^+\big\rangle$. This in fact corresponds to (see equation (26)) $E_M^+(\delta) = |g|\big[J^2 - J\sqrt{(2J + \delta)^2 + 4\tau^2}\big]$, which satisfies $E_M^+(\delta) < E_M^-(\delta)$ for $\delta > 0$. Note that $E_M^-(-|\delta|) \equiv E_M^+(\delta)$. This feature is important because it confirms the symmetry property $\mathrm{e}^{+\mathrm{i}\pi J_1}H_r(\delta)\,\mathrm{e}^{-\mathrm{i}\pi J_1} = H_r(-\delta)$ of repulsive Hamiltonian $H_r(\delta) = -|g|\big(J_3^2 + 2J\tau J_1 + \delta J_3\big)$ stating that the spectra of the cases $\delta > 0$ and $\delta < 0$ must coincide, the relevant Hamiltonians being related by a unitary transformation. Based on this fact, we find as well $\big|E_M^+(\delta)\big\rangle = \mathrm{e}^{+\mathrm{i}\pi J_1}|E_M^-(-|\delta|)\rangle$. By acting with $\mathrm{e}^{\mathrm{i}\pi J_1}$ on $|E_G^-(-|\delta|)\rangle$ we get the expression

$$\big|E_M^+(\delta)\big\rangle = \mathrm{e}^{-\mathrm{i}J_2\phi_-}\,\mathrm{e}^{+\mathrm{i}\pi J_1}|-J\rangle = \mathrm{e}^{\mathrm{i}J\pi}\,\mathrm{e}^{-\mathrm{i}J_2\phi_-}|+J\rangle \tag{30}$$

(note that $\phi_- = \phi_-(-|\delta|)$), where we have used the property of the J_3-basis states $e^{i J_1 \pi}|m\rangle = e^{i J \pi}|-m\rangle$. Upon observing that $\phi_-(-|\delta|) = \phi_+(+|\delta|)$ we conclude that the unitary transformation reproduces, up to a phase factor, the diagonalization-process formula $\left|E_M^+\right\rangle = e^{-i J_2 \phi_+}|+J\rangle$ in a consistent way. Therefore, the ground state of the case $\delta > 0$ is obtained by calculating formula (30) explicitly, which gives

$$\left|E_M^+\right\rangle = \cos^{2J}(\phi_+/2) \sum_{s=0}^{2J} C_{Js} \mathrm{tg}^s(\phi_+/2)|J - s\rangle, \tag{31}$$

where $\phi_+(+|\delta|) = \phi_-(-|\delta|)$. We note that $\left|E_M^+\right\rangle$ corresponds to a coherent state $|+J, \xi\rangle = e^{\xi J_+ - \xi^* J_-}|+J\rangle$ whose extremal state is $|J\rangle$ (instead of $|-J\rangle$) where $|v| = \mathrm{tg}|\xi|$ with $v = -\mathrm{tg}(\phi_-/2)$ reproduces (31). As in the case $\delta < 0$, the remaining state $|E_M^-(\delta)\rangle$ describes the quantum counterpart of the local minimum. The expectation value of J_3 is easily carried out. By using equations (24), one finds that $\left(\langle J_k\rangle_\pm = \left\langle E_M^\pm\right|J_k\left|E_M^\pm\right\rangle, k = 1, 2, 3\right)$ $\langle J_3\rangle_\pm = \langle \pm J|(J_3 \cos\phi_\pm \mp J_1 \sin\phi_\pm)|\pm J\rangle$, $\langle J_1\rangle_\pm = J \sin\phi_\pm$, $\langle J_2\rangle_\pm = 0$, namely

$$\langle J_3\rangle_\pm = \frac{\pm J}{\sqrt{1+\mu_\pm^2}}, \qquad \langle J_1\rangle_\pm = \frac{J\mu_\pm}{\sqrt{1+\mu_\pm^2}}, \tag{32}$$

where $\mu_\pm = 2\tau J/(2J \pm \delta)$, which, expanded up to second order in τ, appear to be consistent with the classical values (A.8) of the minimum-energy configurations. The choice + (−) for the lowest energy state, corresponding to $\delta > 0$ ($\delta < 0$), entails $2J \pm \delta = 2J + |\delta|$ in $\mu_\pm$. Thus $\langle J_3\rangle_+$ and $\langle J_3\rangle_-$ simply differ by a factor −1. In passing, we note that states $\left|E_M^\pm(\delta)\right\rangle$ with the same δ, should satisfy the condition $\left\langle E_M^+\right|E_M^-\rangle = 0$ corresponding to different eigenvalues. $\left|E_M^\pm(\delta)\right\rangle$ obtained within the CMA can be shown to be almost orthogonal[1]. Excited states labelled by $m = \pm(n - J)$ with $n \ll J$ can be derived explicitly from formula (25). By expressing them as $\left|E_m^\pm\right\rangle = U_\pm J_\mp^n|\pm J\rangle/(n!C_{Jn})$, one obtains $\left|E_m^\pm\right\rangle = \left(U_\pm J_1 U_\pm^\dagger \mp i J_2\right)^n \left|E_{\pm J}^\pm\right\rangle/(n!C_{Jn})$, with $U_\pm J_1 U_\pm^\dagger = \cos(\phi_\pm)J_1 \mp \sin(\phi_\pm)J_3$, which can be used to calculate the expectation values of operators $J_k, k = 1, 2, 3$. The condition under which the eigenvalue that corresponds to the local minimum represents the first excited state can be determined quite easily (e.g., for $\delta < 0$) from $E_M^+(\delta) \leqslant E_m^-(\delta)$ with $m = -J + 1$.

Within Fock and Josephson regimes ($\tau < 1$), the AM per boson is readily evaluated from formula (32) giving $\langle \ell_z\rangle = \left[1 \pm (2J \pm \delta)/\sqrt{4\tau^2 J^2 + (2J \pm \delta)^2}\right]/2$. If $\tau \ll 1$, due to $\phi_\pm \simeq 2\tau J/(2J \pm \delta)$ and in view of equations (29) and (30), the ground state reduces to $\left|E_G^\mp\right\rangle \simeq [1 - 2J(\phi_\mp/2)^2][|\mp J\rangle + \sqrt{J/2}\phi_\mp|\mp J \pm 1\rangle]$ where − and + are related to the cases $\delta < 0$ and $\delta > 0$, respectively. Thus in the Fock regime ($\tau \ll 1/J^2$) it is natural to set $\phi_\pm \simeq 0$. By neglecting also the first order corrections, the ground state is approximated by $|E_G(\delta)\rangle = \theta(\delta)|J\rangle + \theta(-\delta)|-J\rangle$ which, when inserted in formula (32), gives $\langle \ell_z\rangle = \theta(\delta) = (1 \mp 1)/2$. This well matches the case $\tau = 0$ where $E_G(\pm|\delta|) = -(|g|J^2 \pm J\Delta)$ with $\delta = \Delta/|g|$.

4. The coherent-state semiclassical approximation

An alternative way to approximate both the ground state and the corresponding energy is to find the quantum counterpart of a classical configuration in terms of coherent states. If the Hamiltonian algebra of a given model is known together with the coherent state relevant to such an algebra, classical variables can be put in a one-to-one correspondence with the

[1] An explicit calculation gives $\langle E_M^+|E_M^-\rangle = [v^2/(1+v^2)]^J$, with $v = \mathrm{tg}[(\phi_+ + \phi_-)/2]$. This term certainly vanishes with $v^2/(1+v^2) < 1$ and $2J = N \gg 1$. Since $v^2/(1+|v|^2) \simeq \tau^2[2J^2/(4J^2 - \delta^2)]$ and $\tau < 1$ then $\langle E_M^+|E_M^-\rangle \to 0$ very rapidly due to the factor τ^{2J}.

complex labels parametrizing a coherent state [21]. This is the case for Hamiltonians (3) and (4) that are written in terms of $su(2)$ generators J_3, $J_\pm$. Coherent states $|-J,\xi\rangle$ of algebra $su(2)$ are defined by equation (27). The latter allows one to parametrize a coherent state by z since $\xi = |\xi|\,\mathrm{e}^{\mathrm{i}\theta}$ is related to $z = |z|\,\mathrm{e}^{\mathrm{i}\theta}$ by $|z| = \mathrm{tg}|\xi|$. For a generic $|z\rangle$ the expectation values $\langle J_k\rangle = \langle z|J_k|z\rangle$, $k = \pm, 3$, given by

$$\langle J_3\rangle = J(|z|^2-1)/(|z|^2+1), \qquad \langle J_+\rangle = 2Jz^*/(|z|^2+1), \tag{33}$$

with $\langle J_-\rangle = \langle J_+\rangle^*$, allow one to determine z when $\langle J_k\rangle$ are known. Note that $\langle J_1\rangle = (\langle J_+\rangle + \langle J_-\rangle)/2$ and $\langle J_2\rangle = (\langle J_+\rangle - \langle J_-\rangle)/2\mathrm{i}$. Therefore classical configurations characterized by known values of J_1, J_2 and J_3 can be associated with a specific z by identifying each classical J_k with $\langle J_k\rangle$ and observing that, owing to equations (27), the phase θ of z coincides with the phase of $J_+ = J_1 + iJ_2$ while $|z|^2 = (J+J_3)/(J-J_3)$. Recalling that this assumption becomes exact in the semiclassical limit $J \to \infty$, we name the map $J_1, J_2, J_3 \to z$ coherent-state semiclassical approximation (CSSA). Determining J_k that characterize the classical energy minimum thus provide the ground-state approximation $|E_M\rangle \simeq |z\rangle$ where $|z\rangle$ is determined by the previous semiclassical map. The corresponding energy is obtained by $E_M^{sc} = \langle z|H|z\rangle$.

5. Conclusions

We have discussed the effectiveness of the CMA based on the Inönü–Wigner transformation by comparing the ground state (GS) obtained in the various regimes of both the repulsive and the attractive models with the exact lowest energy eigenstate determined numerically. In the attractive case ($g < 0$), both for $\tau < 1$ and for $\tau > 1$, and in the repulsive case ($g > 0$) for $\tau > 1$ the CMA leads to approximate X_m of weakly excited states through the eigenfunctions of equivalent harmonic-oscillator problems represented by formulae (10) and (19), respectively. Due to the presence of two classical minima in model (4), the repulsive case with $\tau < 1$ requires that a different diagonalization scheme be developed after implementing the CMA on Hamiltonian (4). This involves weakly excited states represented in terms of $su(2)$ coherent states (29) and (31).

In the attractive case, figure 1 shows that the exact components (calculated numerically) are almost indistinguishable from components X_m obtained within the CMA and described by formula (10). The cases $N = 20$ and $N = 40$ that correspond to $\tau = 0.02 > 1/J^2 = 0.01$ and $\tau = 0.02 > 1/J^2 = 0.0025$, respectively, describe the approach from above to the lower bound of the Josephson regime. In the repulsive case, figure 2 allows one to compare the exact components (calculated numerically) with components X_m obtained within the CMA and described by formula (29) for $\tau = 0.6$ (the Josephson regime), $\nu = 0.8$ and $N = 20, 40$, and by formula (19) for $\tau = 1.6$ (the Rabi regime), $\nu = 0.8$ and $N = 20, 40$. While in the first case formula (29), representing a $su(2)$ coherent state, provides a satisfactory approximation, in the second case formula (19) exhibits a shift on the right of the highest weight components X_m that, in addition, are smaller than the exact ones. In figure 2 (the right panel) X_m evaluated within the CSSA better match the exact ones both qualitatively and quantitatively. When τ is increased (see figure 3), the CMA approximation (CSSA) is satisfactory even if it tends to underestimate (overestimate) exact X_m.

Figures 4 and 5 illustrate, through the parameter $\sigma = \left(E_M^e - E_M^{ap}\right)/\Delta E$, the deviation of the GS energies obtained within the CMA or the CSSA from the GS energy calculated numerically. Energies E_M^e, E_M^{ap} and ΔE are the exact GS energy, the approximated GS energy and the energy range defined as $\Delta E = E_{\max}^e - E_M^e$, respectively. $E_{\max}^e$ is the exact maximum energy. White, light grey and dark grey shades identify the regions in the $\tau\nu$ plane where $\sigma < 0.001$, $0.001 < \sigma < 0.01$ and $0.01 < \sigma < 0.1$, respectively. In figure 4, describing the

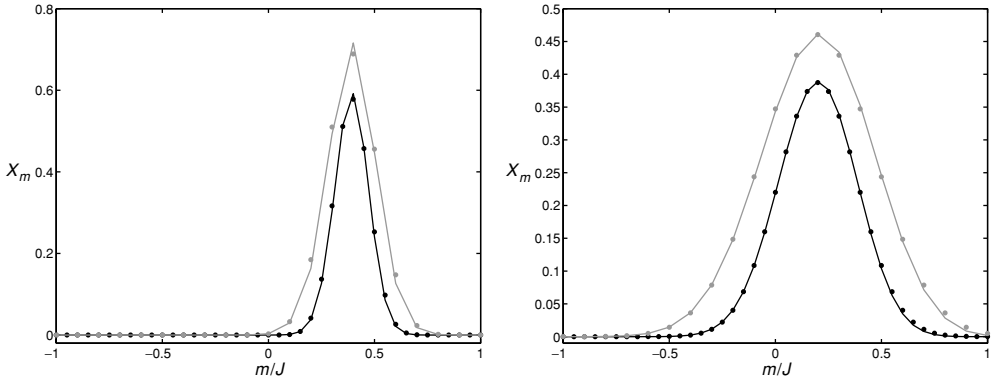

Figure 1. In both panels, grey (dark) diamonds describe the ground-state components X_m, obtained from formula (10), for $N = 20$ ($N = 40$) within the contraction-method approach (CMA). The edges of the grey/dark piecewise-linear curves represent components X_m calculated numerically. Left panel: the Josephson regime in the attractive case with $\tau = 0.02$, $\nu = 0.8$. CMA components X_m and X_m calculated numerically are almost indistinguishable. Right panel: the attractive case with $\tau = 1.0$ (the transition point from the Josephson to Rabi regime) and $\nu = 0.8$. No difference is visible between CMA X_m and X_m calculated numerically.

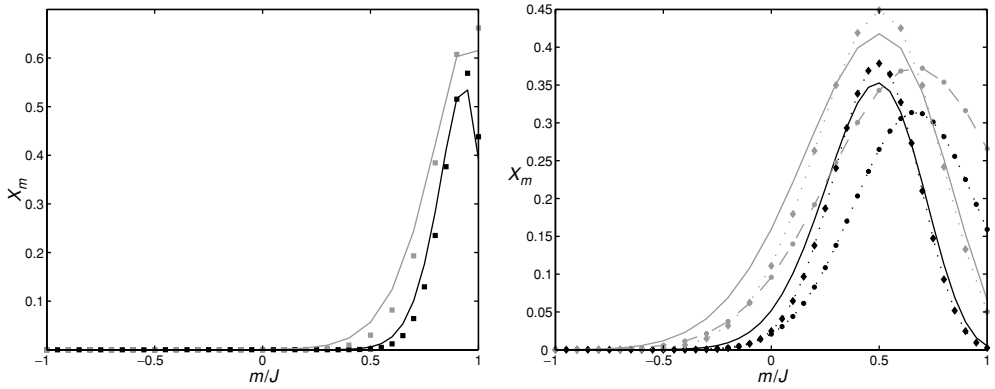

Figure 2. Both panels concern the repulsive case. Grey (dark) squares, diamonds, points and (piecewise-linear, continuous, dotted or dashed) curves are relevant to $N = 20$ ($N = 40$). Left panel: $\tau = 0.6$ (the Josephson regime), $\nu = 0.8$. Within the CMA, the ground-state components X_m, given by formula (29) and described by squares, well approximate the X_m (edges of the grey/dark piecewise-linear curves) calculated numerically. Right panel: $\tau = 1.6$ (the Rabi regime), $\nu = 0.8$. Points (diamonds)—joined by dashed/dotted lines to better distinguish different cases—describe ground-state X_m within the CMA (CSSA) referred to in formula (19) (formula (33)). Continuous piecewise-linear curves represent X_m obtained numerically. The CSSA is qualitatively better than the CMA approximation where curves are shifted on the right. Further comments are given in section 5.

attractive case, E_M^{ap} is given by formula (9). E_M^{ap} well approximates the exact GS energy in the large (white) region in the $\tau\nu$ plane. The repulsive case is considered in figure 5. In the left panel, E_M^{ap} given by formula (18) is shown to well approximate the exact GS energy in a rather restricted region in the $\tau\nu$ plane. In contrast, the right panel shows that evaluating E_M^{ap} based on ground state (33) within the CSSA provides the best approximation ($\sigma < 0.001$) almost everywhere. Concluding, except for the repulsive Josephson regime, where the CMA is not

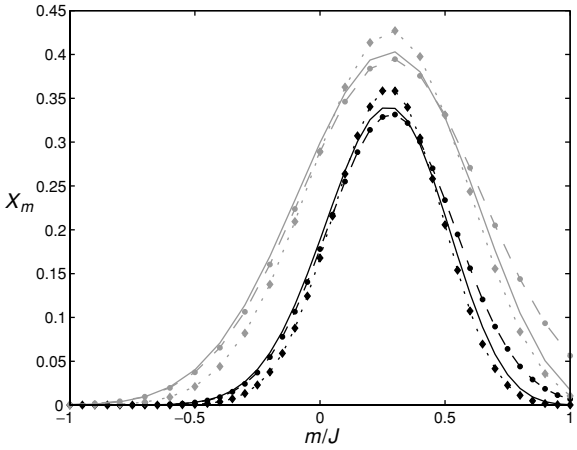

Figure 3. The repulsive case, $\tau = 2.4$ (the Rabi regime), $\nu = 0.8$. Grey (dark) diamonds, points and piecewise-linear curves are relevant to $N = 20$ ($N = 40$). Diamonds (points)—joined by dashed/dotted lines to better distinguish different cases—describe ground-state X_m given by formula (19) (formula (33)) within the CMA (CSSA). Piecewise-linear curves have the usual meaning. Both CSSA and CMA are satisfactory. Further comments are given in section 5.

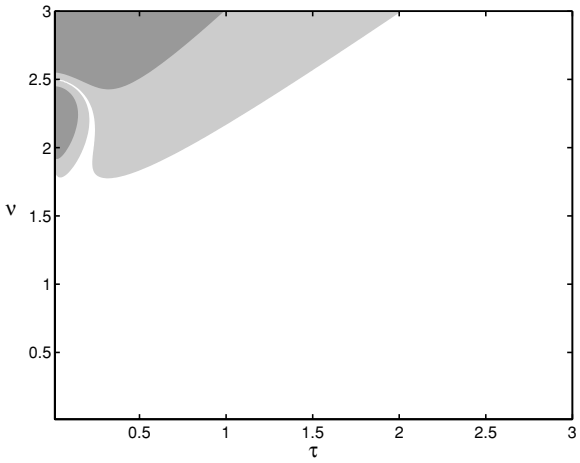

Figure 4. The attractive case. Comparison of the exact ground-state (GS) energy with the ground-state energy (9) within CMA. Different shades in the $\tau\nu$ plane are related to different values of indicator σ. White regions are characterized by an excellent agreement of the exact and the approximated GS energies. See section 5 for details.

satisfactory, both the CMA and the CSSA provide a satisfactory approximation. The CMA is particularly good in the attractive-boson case. Among the many applications to bosonic-well systems currently studied, such approaches seem quite appropriate for studying the low-energy spectrum of the three-well boson systems where the complexity of the energy-level structure mirrors the dynamical instabilities of the chaotic three-well classical dynamics [22]. The study of similar aspects in the three-AM-mode rotational fluid outlined in [3] is currently in progress.

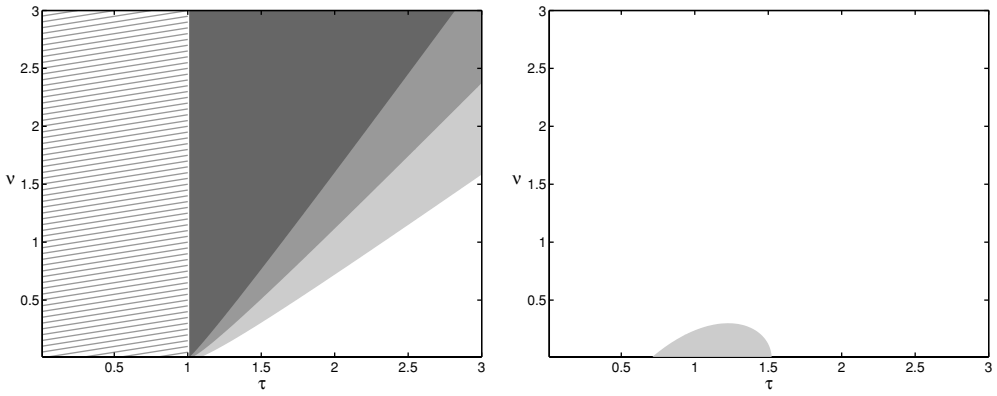

Figure 5. The repulsive case. Comparison of the exact ground-state (GS) energy with approximate GS energies. Different shades in the $\tau\nu$ plane are related to different values of indicator σ. White regions are characterized by an excellent agreement of the exact and the approximated GS energies. Details are discussed in section 5. Left panel: σ for the GS energy (18) ($\tau > 1$). Right panel: σ for the GS energy within the CSSA (the expectation value of H_r for the GS relevant to formula (33)).

Appendix A. Classical energy minima

The classical version of the attractive model (3) displays a dynamics characterized by four (two) fixed points if $1 \gg \tau$ ($\tau \gg 1$). This can be seen by considering the relevant motion equations

$$\dot{J}_1 = (\Delta - 2|g|J_3)J_2, \qquad \dot{J}_3 = -2V_0 J_2, \qquad \dot{J}_2 = 2(|g|J_1 + V_0)J_3 - \Delta J_1, \tag{A.1}$$

equipped with the motion constant $J^2 = J_3^2 + J_2^2 + J_1^2$, which entail the fixed-point equations $J_2 = 0, 2|g|J_3J_1 + 2V_0J_3 - \Delta J_1 = 0$, with the constraint $J^2 = J_3^2 + J_1^2$. Their exact solution involves a fourth-order equation in J_3, except for $\Delta = 0$ when the possible solutions are either $J_1 = -V_0/|g| = -J\tau$ or $J_3 = 0$. In the general case $\Delta \neq 0$, if $1 \gg \tau$ and $J|g| > \Delta > 0$ (namely, for Δ sufficiently small), the searched solutions are such that either $J_3 \simeq \pm J$, $J \gg |J_1|$, or

$$J_1 \simeq \pm J, \qquad J \gg J_3 > 0. \tag{A.2}$$

This feature can be proved explicitly. Particularly, the second pair of solutions is obtained by implementing the approximation $J_1 = s\sqrt{J^2 - J_3^2} \simeq sJ\left(1 - J_3^2/2J^2\right)$, $s = \pm 1$. Neglecting the third-order terms in J_3/J, the second fixed-point equation becomes $(\Delta/2J)J_3^2 + 2J|g|(1 + s\tau)J_3 - J\Delta = 0$, whose roots are found to be $J_3 = 2J\sigma_s^{-1}\left[-1 \pm \sqrt{1 + \sigma_s^2/2}\right]$ with $\sigma_s = \Delta/[J|g|(1+s\tau)]$. While the negative root must be discarded because it entails $|J_3| > J$, the positive root—this can be shown to describe both a minimum ($s = +1$) and a saddle point ($s = -1$)—can be approximated as

$$J_3 \simeq \frac{J\tau\Delta}{2V_0(1 + s\tau)}, \tag{A.3}$$

if $\delta = \Delta/|g| < J$. When $\tau > 1$ (and thus for $\tau \gg 1$) the choices $s = -1, +1$ are related to a maximum and a minimum, respectively. Note that the previous formula giving the J_3 coordinate is well defined for the minimum ($s = +1$) also when $\tau \gg 1$.

Let us consider now the (classical) repulsive model (4). The corresponding Hamiltonian equations read

$$\dot{J}_1 = (\Delta + 2|g|J_3)J_2, \qquad \dot{J}_3 = -2V_0 J_2, \qquad \dot{J}_2 = 2(V_0 - |g|J_1)J_3 - \Delta J_1, \tag{A.4}$$

and exhibit once more the motion constant $J^2 = J_1^2 + +J_2^2 + J_3^2$. For $\Delta = 0$ and $\tau > 1$, the energy minimum is easily shown to correspond to $J_1 = J$, $J_2 = J_3 = 0$. Thus a generic state near the minimum is such that

$$J_1 \simeq J, \qquad |J_2|, |J_3| \ll J. \tag{A.5}$$

If $\Delta \neq 0$, provided $\Delta/J|g|$ is sufficiently small, this statement is certainly valid for $1 \ll \tau = V_0/J|g|$ (the Rabi regime). In fact, by setting $J_1 = \sqrt{J^2 - J_3^2} \simeq J\left(1 - J_3^2/2J^2\right)$ and neglecting the third-order terms in J_3/J in the fixed-point equation $0 = 2(V_0 - |g|J_1)J_3 - \Delta J_1$, one finds that $(\delta/2J)J_3^2 + 2J(\tau - 1)J_3 - \delta J = 0$, whose roots are found to be $J_3 = 2J\alpha^{-1}\left[-1 \pm \sqrt{1 + \alpha^2/2}\right]$, with $\alpha = \Delta/[J|g|(\tau - 1)]$. Discarding the negative root which entails $|J_3| > J$, the positive root can be approximated as

$$J_3 \simeq \frac{\Delta}{2|g|(\tau - 1)} = \frac{J\tau\Delta}{2V_0(\tau - 1)}, \tag{A.6}$$

if $\Delta/J|g| \ll \tau - 1$. In the Rabi regime where $1 \ll \tau \simeq \tau - 1$ such a condition reduces to $\Delta \ll V_0$. In the Fock/Josephson regimes, where $\tau < 1$, the two configurations $J_1 = \tau J$, $J_3 = \pm J\sqrt{1 - \tau^2}$ are found to minimize the energy if $\Delta = 0$. This suggests that, even with $\Delta \neq 0$, low-energy states are such that

$$J_3 \simeq \pm J, \quad |J_2|, \quad |J_1| \ll J. \tag{A.7}$$

To obtain the energy-minimum configurations, in addition to $J_2 = 0$, we consider the second fixed-point equation under the approximation $J_3 = s\sqrt{J^2 - J_1^2} \simeq sJ\left(1 - J_1^2/2J^2\right)$ with $s = \pm 1$. Neglecting the third-order terms in J_1/J, the latter entails $0 = (V_0/J)J_1^2 + (2|g|J - s\Delta)J_1 - 2V_0 J$, which supply, with $s = +1$, two minimum-energy configurations ($\delta = \Delta/|g|$)

$$J_1 \simeq \frac{\tau J}{1 + s\delta/2J}, \qquad J_3 = sJ\sqrt{1 - (J_1/J)^2} \simeq sJ\left[1 - \frac{2J^2\tau^2}{(2J + s\delta)^2}\right]. \tag{A.8}$$

These reproduce correctly the formula of the case $\Delta = 0$.

References

[1] Rokhsar D S 1998 *Preprint* cond-mat/9812260
[2] Leggett A J 2001 *Rev. Mod. Phys.* **73** 307
[3] Ueda M and Leggett A J 1999 *Phys. Rev. Lett.* **8** 83
[4] Kanamoto R, Saito H and Ueda M 2003 *Phys. Rev.* A **68** 043619
[5] Kanamoto R, Saito H and Ueda M 2005 *Phys. Rev. Lett.* **94** 090404
[6] Milburn G J, Corney J, Wright E M and Walls D F 1997 *Phys. Rev.* A **55** 4318
[7] Steel M J and Collett M J 1998 *Phys. Rev.* A **57** 2920
[8] Spekkens R W and Sipe J E 1999 *Phys. Rev.* A **59** 3868
[9] Menotti C, Anglin R, Cirac J I and Zoller P 2001 *Phys. Rev.* A **63** 023601
[10] Mahmud K W, Perry H and Reinhardt W P 2003 *J. Phys. B: At. Mol. Opt. Phys.* **36** L265
[11] Franzosi R, Penna V and Zecchina R 2000 *Int. J. Mod. Phys.* B **14** 943
[12] Benet L, Jung C and Leyvraz F 2003 *J. Phys. A: Math. Gen.* **36** L217
[13] Tonel A P, Links J and Foerster A 2004 *Preprint* cond-mat/0412214
[14] Solomon A I 1971 *J. Math. Phys.* **12** 390
[15] Solomon A I, Feng Y and Penna V 2001 *Phys. Rev.* B **60** 3044
[16] Kostrun M 2004 *Phys. Rev.* A **70** 012105
[17] Inönü E and Wigner E P 1953 *Proc. Natl Acad. Sci. USA* **39** 510

[18] Rowe D J and Thiamova G 2005 The many relationships between the IBM and the Bhor model *Nucl. Phys.* A **760** 59
[19] Gilmore R 1974 *Lie Algebras Lie Groups and Some of Their Applications* (New York: Wiley)
Amico L 2000 *Mod. Phys. Lett.* B **14** 759
[20] Franzosi R and Penna V 2001 *Phys. Rev.* A **63** 043609
[21] Zhang W M, Feng D H and Gilmore R 1990 *Rev. Mod. Phys.* **62** 867
[22] Buonsante P, Franzosi R and Penna V 2003 *Phys. Rev. Lett.* **90** 050404
Pando C L and Doedel E J 2005 *Phys. Rev.* E **71** 056201